Phase Reconstruction Scheme Using Dispersive Media in Direct Detection

Masayuki Matsumoto
Faculty of Systems Engineering, Wakayama University, 930 Sakaedani, Wakayama-shi, 640-8510, Japan
Author e-mail address: mmatsu@sys.wakayama-u.ac.jp

Abstract: A non-iterative reconstruction scheme of phase-modulated signals using dispersive media in direct detection is described. The phase retrieval is performed by solving the temporal transport-of-intensity equation. Required carrier-to-signal power ratio and allowable carrier location in frequency are numerically studied. © 2020 The Author(s)

1. Introduction

Recently a number of research efforts have been devoted to developing phase reconstruction schemes for high-speed complex-modulated optical signals using direct detection (DD). Such DD optical receivers are highly desired for use in simple and low-complexity, but still spectrally-efficient, short and medium reach data transmission systems. One of promising schemes of such receivers is a self-coherent receiver incorporating the Kramers-Kronig (KK) processing, where the signal phase is reconstructed by the Hilbert transform of the logarithm of the signal power waveform under the condition that the signal spectrum has a single-sideband feature with sufficiently high carrier power [1].

Retrieval of phase information of waves from intensity has long been studied in the field of electron microscopy and X-ray and optical imaging [2,3]. Both iterative [4,5] and non-iterative [6] methods have been developed for calculating two-dimensional phase distributions or wave fronts of spatially propagating waves from intensity distributions before and after diffraction. These methods have already been applied in the temporal domain for characterizing short optical pulses in which phase across the pulse is calculated from its intensity waveforms [7-9]. Recently, these phase retrieval methods are being introduced to high-speed optical fiber communications for electrical-domain dispersion compensation and reconstruction of complex-modulated signals in DD optical receivers [10,11]. In [11], the iterative Fresnel-transform Gerchberg-Saxton algorithm was used in an experiment in which dual-polarization QPSK signals without co-transmitted carriers are reconstructed from intensity data detected before and after dispersive elements in the receiver. In this paper, we discuss a non-iterative method of complex signal reconstruction from intensity data based on solution of the temporal transport-of-intensity equation (TIE). Dependence of the reconstruction performance on the carrier-to-signal power ratio and frequency offset between the signal and the carrier is analyzed.

2. Phase extraction based on temporal TIE

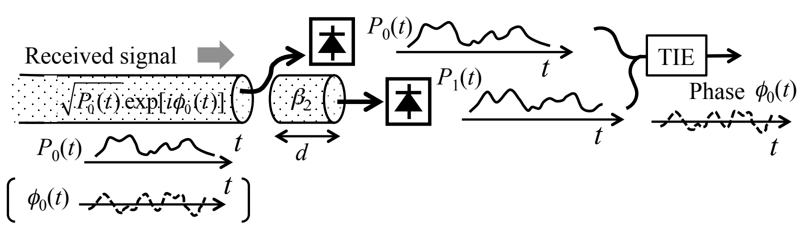

Fig.1. Conceptual diagram of phase extraction based on temporal TIE.

Fig.1 shows a conceptual diagram of the phase extraction using dispersion. The received signal has a power $P_0(t)$ and phase $\phi_0(t)$ and is given by $f_0(t)=P_0(t)^{1/2}\exp[i\phi_0(t)]$, in which $\phi_0(t)$ is lost by the direct detection in measuring $P_0(t)$. To retrieve the phase $\phi_0(t)$, we propagate a part of the signal over a dispersive medium further in the receiver. The propagation of the complex signal $f(t,z)$ in the dispersive medium can be described by $\partial f/\partial z+i(\beta_2/2)\partial^2 f/\partial t^2=0$, where β_2 is the group-velocity dispersion of the medium and $f(t,z=0)=f_0(t)$. The power $P(t,z)$ and the phase $\phi(t,z)$ in the medium, with which $f(t,z)$ is given by $f(t,z)=P(t,z)^{1/2}\exp[i\phi(t,z)]$, satisfy

$$\frac{\partial}{\partial t}\left(P\frac{\partial \phi}{\partial t}\right)=\frac{1}{\beta_2}\frac{\partial P}{\partial z}, \tag{1}$$

which is the one-dimensional temporal TIE [7]. The right-hand side of (1) is approximated by a difference $[P(t,d)-P(t,0)]/(\beta_2 d)=[P_1(t)-P_0(t)]/(\beta_2 d)$, where $P_1(t)$ is the power profile measured after the transmission over a short distance d in the medium.

In the previous study [12], we discretize and transform the left-hand side of (1) from the differential form to a difference form. We solve the resulting linear matrix equation of the form $\boldsymbol{K\Phi}=\boldsymbol{b}$, where $\boldsymbol{K}$ is a tridiagonal symmetric matrix, $\boldsymbol{\Phi}$ is an unknown vector composed of $\phi_0(t=n\Delta t)$ (n=0,1,2,...,N-1), and $\boldsymbol{b}$ is a constant vector corresponding to the right-hand side of (1). In the simulation in this paper, we instead solve (1) using fast Fourier transform, which is computationally more efficient.

3. Numerical examples

We perform numerical simulation of reconstruction of single-polarization Nyquist 16QAM signals using DD and the algorithm based on solving the TIE. For successful signal reconstruction, carrier must be added to the signal as in the KK scheme. The complex amplitude of the transmitted signal is written as

$$E_s(t)=A_0+s(t)\exp(-i2\pi Bt), \tag{2}$$

where A_0 and $s(t)$ are the carrier and complex signal amplitudes, respectively. B represents the frequency offset between the carrier and the signal. In the KK scheme B is chosen to be equal to a half of the baud rate, meaning that the carrier is located at one edge of the signal spectrum. In our case, the carrier can be located within the signal spectrum. Fig.2 shows a schematic diagram of the receiver. The incoming signal is detected by two photodiodes one of which detects the signal after an optical dispersive element. Suitable delay either in the optical or electrical domain is needed in one of the branch to align in time the two detected signals.

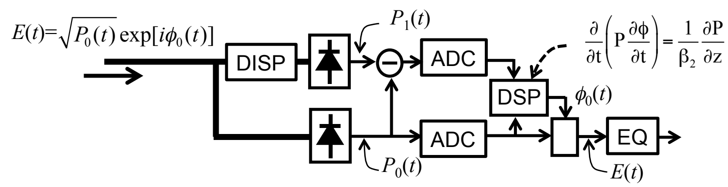

Fig.2. Schematic diagram of the DD receiver. DISP: dispersive element, EQ: equalization.

In the simulation 10 GBaud Nyquist 16QAM signals together with a carrier is assumed to be transmitted over a standard single-mode fiber (SSMF). Nonlinear effects in the transmission fiber are neglected. Gaussian noise with bandwidth of 12.5 GHz is added to the signal before detection. The dispersion given to the signal inside the receiver for phase extraction is 50 ps/nm. The electrical signal processing for the phase extraction, which is performed on every block of 1024 symbols, is assumed ideal in the current simulation. The dispersion of the transmission fiber is compensated in the electrical domain after the signal is reconstructed. Quality of the reconstructed signal is evaluated in terms of error vector magnitude (EVM) that is defined as the ratio of the variance of error to the average power in the constellation diagram. Symbol error rate (SER) is also calculated.

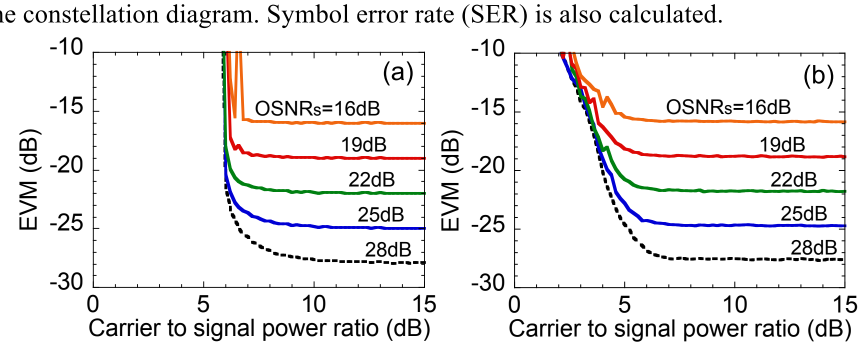

Fig.3. EVM versus CSPR for (a) TIE-based reconstruction and (b) KK-based reconstruction. Frequency offset B=6 GHz in the KK-based reconstruction. $OSNR_s$ does not include carrier power in the signal power.

Firstly, back-to-back reconstruction performance versus the carrier power is examined. The carrier is located at the center of the signal spectrum, or B is equal to zero in (2). Fig.3(a) shows EVM in the unit of dB versus the carrier to signal power ratio (CSPR) for different optical signal to noise ratios. The OSNR (denoted as $OSNR_s$) considers only the single-polarization noise and excludes the carrier power. In the case of Nyquist signals and no signal degradation other than noise, EVM of the signal is given by $EVM=B_n/(B_{ref}\ OSNR_s)$, where B_n is the bandwidth of the added noise and B_{ref} is the reference noise bandwidth for the OSNR definition. Because

B_n=B_{ref}=12.5GHz in the current simulation, EVM is equal to 1/OSNR$_s$, or EVM[dB]=-OSNR$_s$[dB], in the absence of reconstruction error. This is indeed shown in Fig.3(a) when CSPR is larger than about 10dB. For smaller CSPRs, the power of the optical signal together with noise can be close to zero at some instance in the 1024-symbol signal block. When this event happens or the trajectory of the complex signal encircles the origin in the complex plane, the reconstruction fails. Similar behavior appears also in the signal reconstruction using the KK method as shown in Fig.3(b). In the reconstruction using TIE, EVMs are increased abruptly at CSPR about 7dB, which indicates that the requirement for the CSPR is more stringent in the TIE-based reconstruction.

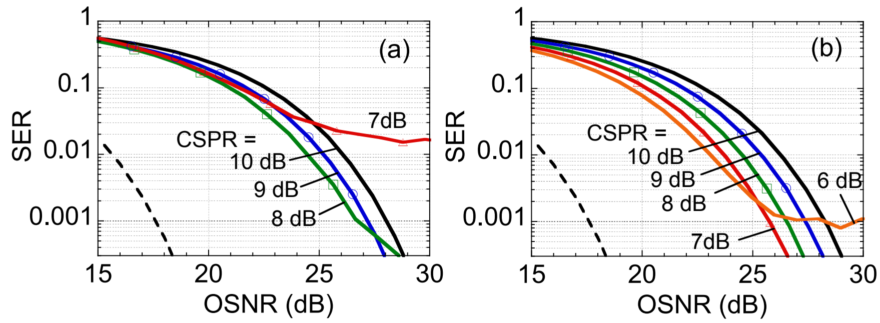

Fig.4. SER versus OSNR for (a) TIE-based reconstruction and (b) KK-based reconstruction. B=0 and 6GHz in (a) and (b), respectively. OSNR in horizontal axes includes the carrier power and is related to OSNR$_s$ as OSNR=(1+CSPR) OSNR$_s$. The dashed curve shows the theoretical SER for the coherent receiver.

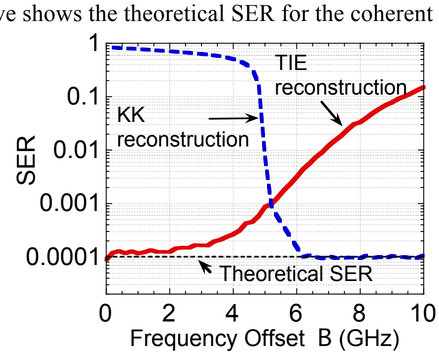

Fig.5. SER versus location of the carrier frequency in the signal spectrum.

Fig. 4(a) and (b) show symbol error rates after transmission of 100km SSMF for TIE and KK-based signal reconstruction schemes, respectively. In accordance with the behavior seen in Fig.3, the performance of the TIE-based receiver is worse than the KK receiver by about 2dB in terms of OSNR requirements.

An advantage of the TIE-based DD receiver over the KK receiver is that the carrier frequency can be located inside the signal spectrum. Fig. 5 shows SER after 100km transmission and detection using TIE and KK-based receivers when the frequency difference between the carrier and signal, B in (2), is varied. CSPR and OSNR$_s$ are 10dB and 19dB, respectively. It is shown that the SER is the smallest when B=0 for the TIE-based reconstruction. For KK-based reconstruction, on the other hand, single-side band condition is strictly required. This indicates that the TIE receiver has larger flexibility in the spectral shape or the modulation format of the signal to be used.

4. Conclusion

Phase reconstruction from power waveforms by solving the temporal transport-of-intensity equation is described. Features of the reconstruction scheme are compared with the KK method. Studies of practical issues such as required sampling rate in the reconstruction signal processing and optimum values of the dispersion in the receiver are needed.

References

[1] A. Mecozzi, C. Antonelli, and M. Shtaif, Optica **3**, 1220 (2016). [2] K. A. Nugent, D. Paganin, and T. E. Gureyev, Phys.Today, Aug. 2001, 27 (2001). [3] Y. Shechtman, Y. C. Eldar, O. Cohen, H. N. Chapman, J. Miao, and M. Segev, IEEE Sig. Proc. Mag., May 2015, 87 (2015). [4] R. W. Gerchberg and W. O. Saxton, Optik **35**, 237 (1972). [5] J. R. Fienup, Opt. Lett. **3**, 27 (1978). [6] M. R. Teague, J. Opt. Soc. Am. **73**, 1434 (1983). [7] C. Dorrer, Opt. Lett. **30**, 3237 (2005). [8] D. R. Solli, S. Gupta, and B. Jalali, Appl. Phys. Lett. **95**, 231108 (2009). [9] C. Cuadrado-Laborde, A. Carrascosa, P. Pérez-Millán, A. Díez, J. L. Cruz, and M. V. Andres, Opt. Lett. **39**, 598 (2014). [10] G. Goeger, C. Prodaniuc, Y. Ye, and Q. Zhang, ECOC2015, P.3.12 (2015). [11] H. Chen, N. K. Fontaine, J. M. Gené, R. Ryf, D. T. Neilson, and G. Rabon, ECOC2019, Tu.1.D.1 (2019). [12] M. Matsumoto, CLEO2018, STu3C.5 (2018).